Aust. J. Phys., 1984, **37**, 263–6

Refraction in Elastic Collisions of Heavy Ions

C. B. O. Mohr

School of Physics, University of Melbourne,
Parkville, Vic. 3052.

Abstract

We attempt to improve our understanding of the processes of absorption and refraction in heavy-ion elastic collisions. The WKB method for a complex potential provides a link. The results account for certain observed features of the scattering angular distributions.

1. Introduction

In our last paper (Mohr 1984) we summarized and classified some points in the strong absorption theory of elastic collisions, and here we extend our treatment and include the effect of refraction, which has hitherto not received altogether satisfactory treatment. The effects of absorption and refraction are in fact linked, and it is through investigation of the link that the solution of the problem appears. This involves using the WKB method for a complex potential.

2. Strong Absorption—The Coulomb Potential

We start with the fundamental relation

$$k \sin\tfrac{1}{2}\theta f^{\pm}(\theta) = c \int_{-\infty}^{\infty} S(\lambda) \exp(-\mathrm{i}\lambda\theta^{\pm})\, \mathrm{d}\lambda, \tag{1}$$

with

$$S(\lambda) = 1/\{1+\exp(-\lambda/\Delta)\}, \tag{2}$$

where $c = -(l_c/2\pi)^{\frac{1}{2}}$, $\lambda = l - l_c$ and $\theta^{\pm} = \theta \pm \theta_c$.

We showed in our last paper (Mohr 1984) that

$$k \sin\tfrac{1}{2}\theta f^{\pm}(\theta) = \mathrm{i}c\pi\Delta/\sinh(\pi\Delta\theta^{\pm}), \tag{3}$$

which diverges as $\theta^{\pm} \to 0$, so that (3) cannot be used for $f^{-}(\theta)$ for $\theta < \theta_c$; otherwise f^{+} and f^{-} are similar functions in the absence of refraction.

We have in the past made much use of the phase–amplitude diagram, and in our previous paper (see Fig. 3) we showed its general form, which is a spiral terminating at a point T, where O′T is the value of (1) for $\lambda \to -\infty$, and O′ is the origin of the

0004-9506/84/030263$02.00

complex space. The spiral structure cannot be seen properly on a linear scale, only on a logarithmic scale, because $\int_{\lambda}^{\infty} S(\lambda)\exp(\pm i\lambda\theta^{\pm})$ tends to small values very rapidly as $\lambda \to -\infty$.

This may be seen as follows. Writing for convenience $\beta = 1/\Delta$, we have from (2)

$$\begin{aligned} S(\lambda) &= 1/\exp(-\beta\lambda)(\exp\beta\lambda + 1) \\ &= \exp\beta\lambda(1 - \exp\beta\lambda + \exp 2\beta\lambda - \ldots) \\ &= \exp\beta\lambda - \exp 2\beta\lambda + \exp 3\beta\lambda - \ldots, \end{aligned} \tag{4}$$

which is convergent for $\lambda < 0$ (or $l < l_c$). Hence, we have

$$\int_{-\infty}^{\lambda} S\exp(-i\lambda\theta^{-})\,d\lambda = \{\exp\beta\lambda/(\beta - i\theta^{-}) - \exp 2\beta\lambda/(2\beta - i\theta^{-}) + \ldots\}\exp(-i\lambda\theta^{-}), \tag{5}$$

which can easily be separated into real and imaginary parts. For $\lambda < -2$ the first term of this series usually gives sufficient accuracy. This term tends to zero as $\lambda \to -\infty$, but we expect its value to approach the finite quantity (3) as $\lambda \to -|\lambda_t|$, a terminal value. It is of interest to determine the value of $|\lambda_t|$. We note that for $\Delta\theta^{-} > 2$, the value of $k\sin^{\frac{1}{2}}\theta f^{-}$ from (3) is nearly $ic\pi\exp(-\pi\Delta\theta^{-})$. Comparing this with the magnitude of the first term of (5), namely $c\{\beta^2 + (\theta^{-})^2\}^{-\frac{1}{2}}\exp(-\beta|\lambda|)$, we see that

$$|\lambda_t| = b + \Delta^2\theta^{-}, \tag{6}$$

where $b = \frac{1}{2}\ln\{1 + (\Delta\theta^{-})^2\} + \ln(\pi/\Delta)$, which is usually of order unity.

Because of the divergence of (3) at $\theta^{-} \to 0$ it is not safe to use (3) for $\theta^{-} < 1$. Now Δ lies between about 1 and 3 for all but the very lighter pairs of heavy ions (Mohr 1979, Fig. 4). So we see from (6) that the value of λ_t is usually a two-digit number.

3. Effect of the Nuclear Potential—Real Phases

It is inclusion of the nuclear potential which gives the differences between f^{+} and f^{-}. To fix our ideas we shall consider the particular case of ${}^{40}_{18}\mathrm{Ar} + {}^{120}_{50}\mathrm{Sn}$, discussed by Glendenning (1975, Section 6) and illustrated in his Fig. 15. Some of the information is presented in our Fig. 1 a little differently.

The horizontal line marks the centre-of-mass energy, the sloping lines show the value of $(V_C + V_L)^{\frac{1}{2}}$ for different values of $V_L = l(l+1)\hbar^2/2mr^2$ and the portion of the Woods–Saxon potential well shows $V_N^{\frac{1}{2}}$, where V_N is the real nuclear potential. The dashed vertical lines indicate the successive areas added as l is decreased in steps of 20 units, when the WKB method is used to calculate the change in the real phase due to V_N alone. We are not concerned with the value of the real phase due to $V_C + V_L$, for this is taken to be θ_c for all values of l in the theory of strong absorption.

4. Coupling between Real and Imaginary Phases

For a complex potential which does not vary too rapidly, a modification of the WKB method can give useful results (Mohr 1957). When used for 4 MeV nucleons incident on a heavy nucleus the complex potential gives fluctuations in the values of the real and imaginary parts of the phases when compared with accurate calculations,

but it should be satisfactory for heavy ions where the number of partial waves l is very much larger.

We consider the radial equation for the partial wave of order l

$$d^2u/dr^2 + (U + i\,W)u = 0,$$

where $U = E + V + i\,W_N$, with V including all real potential energy terms including V_L and V_N. We write $(U + i\,W)^{\frac{1}{2}} = P + i\,Q$, where the principal values of P and Q are taken. This procedure takes account of the coupling between the real and imaginary parts of u. Then the real and imaginary parts of the phase are given approximately by $\int^r P\,dr$ and $\int^r Q\,dr$ respectively. Again we are interested only in the change of phase produced by the nucleon potential $V_N + i\,W_N$, and when we evaluate $\int^r Q\,dr$ for different values of l split the area under the curve for Q into successive vertical strips as we did for $V_N^{\frac{1}{2}}$ in considering the nuclear potential to be purely real.

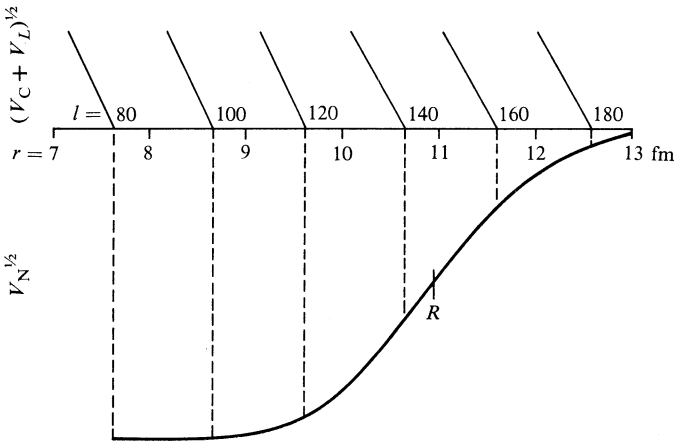

Fig. 1. Part of the effective potential for $^{40}_{18}Ar + ^{120}_{50}Sn$. The centre-of-mass energy is shown by the horizontal line. A portion of the real potential well is shown by the solid curve. Here R is the nuclear radius. (See Section 3.)

Referring to Fig. 1, we find that penetration to the point R, at an ion separation distance of 11 fm, occurs for a value of $|\lambda_t|$ of about 40, and the calculated change in the real phase is of the order of a couple of radians; but most of this change occurs near the terminal point of the spiral after several terms of the spiral have reduced its size, and the effect is probably not important.

5. Refraction—Imaginary Phases

More important than the real phase is the change in the imaginary phase produced by the imaginary nuclear potential, and moreover the effect is readily quantifiable. Following the splitting of the area under the curve in Fig. 1 into vertical strips, we see that the change of phase with distance parallels the change of potential with distance, for the real and the imaginary potentials are usually taken to be of the same form. Glendenning (1975) took the form $\{1 + \exp(r - R)/a\}^{-1}$ with $a = 0{\cdot}45$ fm, and for points to the right of R this form tends more and more nearly to $\exp(-r/a)$. However, we are more interested in the change with respect to l (or λ), namely

$\exp(-|\lambda|/a')$, and we see that the scales of l and r are in the ratio of about 20 to 1, so that $a' = 9$ fm.

Without refraction the dominant term on the right-hand side of (4) is $\exp\beta\lambda$, or $\exp(-|\lambda|/\Delta)$, and with refraction this becomes $\exp(-|\lambda|/\Delta^{\pm})$. We are interested in the fractional rate of change of these two quantities and $\exp(-|\lambda|/a')$ with respect to λ (logarithmic derivative), and so we have

$$1/\Delta^{\pm} = 1/\Delta \pm 1/a' . \tag{7}$$

6. Discussion

This final relation (7) gives reasonable values for Δ^{+} and Δ^{-}; and we can see why they are energy-dependent. At a higher energy the lines of different l in a diagram like Fig. 1 will be steeper and closer together, so that for the same a the value of a' will be smaller, making $\Delta^{-} - \Delta^{+}$ greater. Also, for the same projectile energy but different target nuclei, Δ^{+} and Δ^{-} will be about the same. These two general results have been observed (Mohr 1979, Section 2) but not hitherto clearly understood.

A result different from (7) has been obtained by Rowley and Marty (1976), using considerations of saddle-points and poles in the complex angular momentum plane, and a parametrization of the nuclear phase not related to the nuclear interaction (see Mohr 1979, equation 5).

Recent work on the $^{16}O+^{16}O$ optical potential by Sartor and Stancu (1983) showed that while the real and imaginary parts are of appreciably different form at smaller distances, and are strongly energy-dependent, they are of the same form near the nuclear surface. Of course the diffuseness a may show variations in its value due to shell effects.

References

Glendenning, N. K. (1975). *Rev. Mod. Phys.* **47**, 659.
Mohr, C. B. O. (1957). *Aust. J. Phys.* **10**, 110.
Mohr, C. B. O. (1979). *Aust. J. Phys.* **32**, 541.
Mohr, C. B. O. (1984). *Aust. J. Phys.* **37**, 9.
Rowley, N., and Marty, C. (1976). *Nucl. Phys.* A **266**, 494.
Sartor, R., and Stancu, F. (1983). *Nucl. Phys.* A **404**, 392.

Manuscript received 26 January, accepted 5 April 1984